# CHANGES IN INTER-LIMB MUSCLE COORDINATION INDUCED BY MUSCLE FATIGUE DURING PEDALING

**Takuhiro Sato, Shota Shigetome, and Tatsushi Tokuyasu**

**Department of Engineering, Fukuoka Institute of Technology, Fukuoka, Japan**

The purpose of this study was to investigate the changes in inter-limb muscle coordination brought about by muscle fatigue during pedaling. Four healthy male road cyclists pedaled for 15 min under a 150 W exercise load and a 90 rpm cadence. First, the surface electromyography (sEMG) of the muscles of both lower limbs was measured along with crank angle. Second, the slope of median frequency of a short-time Fourier transform was used to estimate muscle fatigue. Next, non-negative matrix factorization was applied to the time-frequency components of the sEMG to investigate the inter-limb muscle coordination. The result showed that asymmetrical inter-limb muscle coordination was seen in all subjects regardless of muscle fatigue. Failure to counteract muscle fatigue could be explained by the redistribution patterns of the asymmetrical inter-limb muscle coordination, which is considered a muscle fatigue compensation strategy.

**KEYWORDS:** muscle fatigue, cycling, surface electromyography, muscle coordination.

**INTRODUCTION:** In a cycling competition, counteracting the effects of muscle fatigue modifies muscle coordination to improve the efficiency of pedaling (Blake & Wakeling, 2015; Enoka & Stuart, 1992). Generally, muscle fatigue is a reduction in the muscle's capability to generate force, as well as a change in both the level and shape of muscle activity due to exercise (Gandevia, 2001). Related research has identified that the interindividual variability of surface electromyography (sEMG) observed during pedaling does not represent differences in the neural strategy for pedaling (Hug, Turpin, Guével, & Dorel, 2010). This is because the sEMG observed during pedaling is affected by changes in cadence, workload, and riding posture. On the other hand, muscle synergy is considered a neural strategy for simplifying neuromuscular commands, which show robustness against the changes of cadence, workload, and riding posture (Hug, Turpin, Couturier, & Dorel, 2011). The synergy can be obtained from the sEMG recorded from numerous muscles via decomposition algorithms, such as non-negative matrix factorization (NMF) (D'avella, Saltiel, & Bizzi, 2003). Related research has also shown that, for trained cyclists, pedaling is accomplished by combining a few muscle synergies (Hug et al., 2011). Nevertheless, the present understanding of muscle coordination is limited to a single lower limb (Sato & Tokuyasu, 2017; Taborri et al., 2018). The authors consider that gaining insight into the prevention of muscle fatigue needs to include consideration of asymmetrical muscle coordination in both the left and right lower limbs. Therefore, the aim of this study was to investigate the changes in inter-limb muscle coordination, based on muscle synergy, arising from muscle fatigue during pedaling. The results of the current study could contribute to the interpretation of the relationship between localized muscle fatigue and asymmetrical muscle coordination for improving cyclists' performance.

## METHODS:

**Subject and experimental protocol:** Four healthy male road cyclists participated in the experiment (age: 34.8±9.84 years, height: 1.72±3.9 m, body mass: 67.1±8.3 kg, cycling experience: 8.5±3 years, dominant leg: right). Verbal and written informed consent was obtained before the experiment. The experimental device consisted of a road bike (RS8, Bridgestone anchor), clipless pedals (PD-5800, Shimano), a rotary encoder (E6C2-CWZ1X, Omron), and a power meter (Power Tap SL+, CycleOps). The rotary encoder detected the crank angle by using a belt connected to the crank's rotor. Both cadence and workload were measured using a cycle computer (Edge 800J, Garmin). A wireless myoelectric probe (FREEEMG 1000, BTS Bioengineering Corp) with an electrode (H124SG, Covidien) was used to measure sEMG. Heart rate (HR) was measured using an optical HR sensor (A370, Polar) at 1 Hz. The crank angle and sEMG were simultaneously measured at 1k Hz. Figure 1(a)

shows the 10 muscles in the left and right lower limbs that were measured: Tensor fasciae latae (TFL), Rectus femoris (RF), Biceps femoris (BF), Tibialis anterior (TA), and Gastrocnemius medialis (GM). For elimination of both noise from the power supply and motion artifacts, a Ham filter (60 Hz) and a bandpass filter (15–490 Hz) were applied to the sEMG. The experiment was conducted in a laboratory at 21 °C with 65% humidity. The subjects were instructed to pedal under a 150 W exercise load with a 90-rpm cadence for 15 min. The experiment was terminated when the subject's HR exceeded 80% of the maximum HR estimated by the Karvonen formula (Robergs & Landwehr, 2002). The exercise load was adjusted using the gear ratio. The subjects warmed up via a pedaling exercise in the laboratory 1 hr before the experiments began and adjusted the saddle height to their own preferred height. During the experiment, the subjects grasped the middle of the handlebar.

**Muscle fatigue estimation and muscle synergy analysis:** A median frequency (MDF) obtained using the short-time Fourier transform (STFT) method of sEMG reported the tendency of muscle fatigue during dynamic contractions, and the MDF slopes of the sEMG reported the level of muscle fatigue (Dingwell, Joubert, Diefenthaeler, & Trinity, 2008). Therefore, MDF slopes were computed every 45 cycles to determine the effect of muscle fatigue on muscle coordination changes between the lower limbs. The time frequency component of the sEMG reflects the changes in the muscle fibers' frequency and timing of firing (Tscharner, 2000). Thus, as shown in Figure 1(b), the sEMGs were processed across a wavelet filter bank, a set of nine wavelets with center frequencies (CF) in the range of 19–330 Hz, with a nonlinear scaled function according to the equation

$$\psi_j = \frac{1}{\text{scale}} \cdot (j + q)^r$$

where $\psi_j$ is the CF of #*j* wavelet (Hz), scale = 0.3 defines a range of frequencies provided by different wavelets, and $q$ = 1.45 and $r$ = 1.959 optimize the spacing between the wavelets (Tscharner et al., 2000). From the above, the wavelet power spectrums were obtained by calculating inverse Fourier transform (IFT) to the multiplication of both the sEMG and wavelets in the FFT domain, and their root mean squared (RMS) values were calculated with the time interval required for the 5 deg crank angle. The RMS wavelet power spectrums were concatenated across 45 cycles to create the matrix, ***M***, for muscle synergy extraction, as shown in Figure 1(c). After normalizing ***M*** by peak value per muscle, NMF was applied. In the NMF, muscle synergy was extracted from ***M*** by minimizing the Frobenium norm between ***M*** and ***C*×*W***: the synergy activation coefficient ***C*** (***m*** by ***s***) $\geq$ 0 and synergy vector ***W*** (***s*** *by* ***n***) $\geq$ 0. In neurophysiological terms, this means that the synergy activation coefficient represents the muscle activity level and timing via the central nervous system (CNS), whereas the synergy vector represents the muscle coordination via the CNS (D'avella et al., 2003). Knowing the number of synergies, ***s***, that determine the dimensions of ***C*** and ***W*** is key to understanding the extent to which the CNS dominates a set of grouped muscles. Finally, ***s*** was chosen by means of variance accounted for (VAF) per muscle, which is defined by the percentage obtained by subtracting 1 from the non-centered Pearson's moment correlation coefficients of an input signal. This means that VAF per muscle returns values for ***s*** that sufficiently reconstruct the input signal in spite of dimensional reduction. For this study, the synergy value at which the mean VAF across all muscles reached 80% was chosen (Ortega-Auriol, Besier, Byblow, & McMorland, 2018).

## RESULTS:

**Muscle fatigue during pedaling:** Figure 2 shows the MDF slopes of the sEMG for all subjects. The slopes' negative values indicate the muscle fatigue level, which varies between the subjects for $TFL_R$, $RF_R$, and $BF_R$ on the right leg and $RF_L$, $BF_L$, and $TA_L$ on the left leg. Subject 1 was chosen as the most useful result because he was unable to finish the protocol due to muscle fatigue.

**The effect of muscle fatigue on muscle synergy:** For 45 cycles in 30 s at the start (non-fatigued) and end (fatigued), the results of both the synergy vector W and the mean of synergy activation coefficient in the cycles, $\bar{\boldsymbol{C}}$, are shown in Figures 3(a) and 3(b), respectively. The

number of synergies was reduced from four at the start to three at the end. For synergy #1, the value of $\boldsymbol{W}$ in the left lower limb muscles slightly increased, and $\bar{\boldsymbol{C}}$ increased when the right pedal was around 90 deg. A similar result was found for synergies #2 in the non-fatigued state and #3 in the fatigued state. The value of $\boldsymbol{W}$ for the right lower limb muscles decreased at synergy #2 in the non-fatigued state, while the value of $\boldsymbol{W}$ for the left lower limb muscles increased at synergy #3 in the fatigued state. The $\boldsymbol{W}$ values were mainly redistributed to the left lower limb and the peak of $\bar{\boldsymbol{C}}$ shifted slightly forward. A similar synergy was found between synergy #3 in the non-fatigued state and synergy #2 in the fatigued state. For all subjects, both $\boldsymbol{W}$ and $\bar{\boldsymbol{C}}$ of the lower extremities increased in the fatigued condition with the peak of $\bar{\boldsymbol{C}}$ shifting forward. Overall, the forward peak shift of $\bar{\boldsymbol{C}}$ was confirmed for all subjects, while the $\boldsymbol{W}$ values were mainly redistributed to both lower limbs, which was only seen in subject 1.

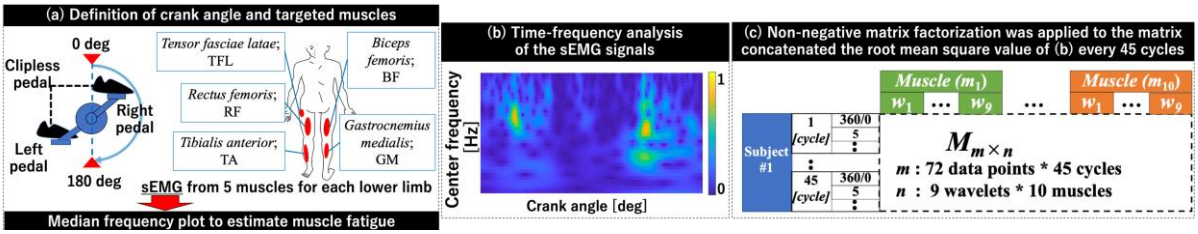


**Figure 1: Example of sEMG processing.** (a) Crank angle definition. The initial crank angle was defined as 0 deg and 180 deg, and the clockwise crank rotation was defined as positive. The muscles of both the left and right lower limbs were measured. (b) The sEMG results of both lower limbs were transformed into their time-frequency component by a wavelet bank, representing the change in the wavelet power spectrum with CF in the range of 19–330 Hz (19.29, 37.71, 62.09, 92.36, 128.48, 170.39, 218.08, 271.50, 330.63 Hz), #1–#9 wavelet. (c) The wavelet power spectrums were RMS of the crank angle for every 5 deg (72 data points), depicted as “360/0”, “5”, etc. The spectrums’ RMS concatenated every 45 cycles to create the NMF matrix. The $\boldsymbol{M}$ consists of *m* rows by *n* columns: *m* represents the data points for all 45 cycles, and *n* represents the 9 wavelets * 10 muscles.

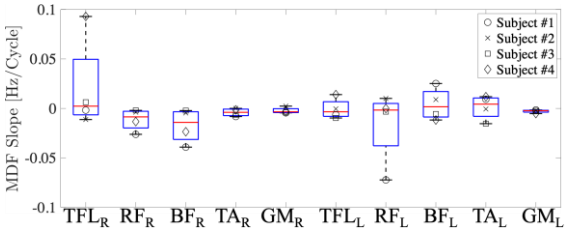


**Figure 2: Boxplot of the MDF slopes of sEMG for all subjects.** The red line in each box shows the median slope for all subjects. On the Y-axis, the negative values indicate muscle fatigue. The X-axis shows the right (R) and left (L) lower limb muscles. Each symbol in the legend represents an individual subject.

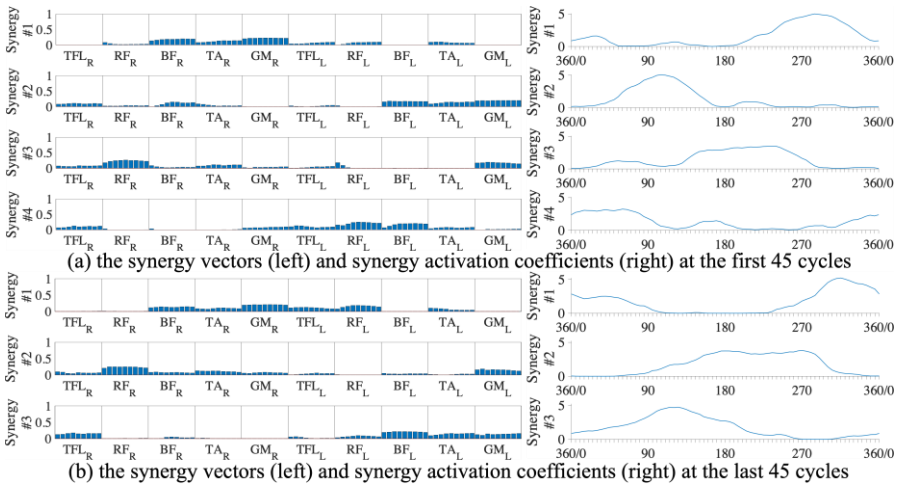


**Figure 3: Muscle coordination between the lower extremities for subject 1.** (a) and (b) represent non-fatigued and fatigued conditions, respectively. The left panel of each shows the synergy vectors $\boldsymbol{W}$,

which represent muscle coordination, and the X- and Y-axis represent wavelets #1–#9 of each muscle and the number of synergies, respectively. The right panel of each shows the mean synergy activation coefficients $\bar{\boldsymbol{C}}$, which represent the activation timing of muscle coordination for 45 cycles, and the X- and Y-axis represent the crank angle and the number of synergies, respectively.

**DISCUSSION:** Although asymmetrical inter-limb muscle coordination was confirmed in all subjects, the redistribution of $\boldsymbol{W}$ could be an important factor for understanding their individual pedaling strategies to counteract muscle fatigue. It has been reported that motor adaptation to muscle fatigue indicates a peak shift in the synergy activation coefficient, as well as a slight adjustment of the synergy vector during pedaling (Hug et al., 2011). These muscle synergy adjustments were confirmed only in the subjects who could finish the protocol. In regard to the reduction in the number of synergies, which was caused by muscle fatigue, one related study on the relationship between number of synergies and motor task performance reported that a reduction in the number of synergies in post-stroke individuals on their paretic side indicates impairments in lower-limb muscle coordination (Taborri et al., 2018). The authors considered that both the number of synergies and the synergy vector redistribution between the lower limbs after muscle fatigue, which was seen only in subject 1, indicated a lack of adaptability to maintain muscle coordination. Although the fatigued and non-fatigued conditions were compared to investigate the effects of muscle fatigue, a variable number of synergies could be needed to explain the redistribution process of muscle coordination patterns seen in the synergy vectors across whole cycles. This approach could provide better insight into localized muscle fatigue prevention.

**CONCLUSION:** A synergy activation coefficient peak shift was confirmed for all subjects, while a synergy vector redistribution was seen only in the subject who suffered from muscle fatigue. Failure to counteract muscle fatigue could be explained by the redistribution patterns of asymmetrical muscle coordination between the lower limbs, which indicates the use of a pedaling strategy to compensate for muscle fatigue.

## REFERENCES:

Blake, O. M. & Wakeling, J. M. (2015). Muscle coordination limits efficiency and power output of human limb movement under a wide range of mechanical demands. *Journal of Neurophysiology*, *114*(6), 3283–3295.

D'avella, A., Saltiel, P., & Bizzi, E. (2003). Combinations of muscle synergies in the construction of a natural motor behavior. *Nature Neuroscience*, *6*(3), 300–308.

Dingwell, J., Joubert, J., Diefenthaeler, F., & Trinity, J. (2008). Changes in muscle activity and kinematics of highly trained cyclists during fatigue. *IEEE Transactions on Biomedical Engineering*, *55*(11), 2666–2674.

Enoka, R. M. & Stuart, D. G. (1992). Neurobiology of muscle fatigue. *Journal of Applied Physiology*, *72*(5), 1631–1648.

Gandevia, S. C. (2001). Spinal and supraspinal factors in human muscle fatigue. *Physiological Reviews*, *81*(4), 1725–1789.

Hug, F., Turpin, N. A., Couturier, A., & Dorel, S. (2011). Consistency of muscle synergies during pedaling across different mechanical constraints. *Journal of Neurophysiology*, *106*(1), 91–103.

Hug, F., Turpin, N. A., Guével, A., & Dorel, S. (2010). Is interindividual variability of EMG patterns in trained cyclists related to different muscle synergies? *Journal of Applied Physiology*, *108*(6), 1727–1736.

Ortega-Auriol, P. A., Besier, T. F., Byblow, W. D., & McMorland, A. (2018). Fatigue influences the recruitment, but not structure, of muscle synergies. *Frontiers in Human Neuroscienc*e, *12*(217).

Robergs, R. A. & Landwehr, R. (2002). The surprising history of the "HRmax=220-age" equation. *Journal of Exercise Physiology*, *5*(2), 1–10.

Sato, T. & Tokuyasu, T. (2017). Pedaling skill training system with visual feedback of muscle activity pattern. *Journal of Biomechanical Science and Engineering*, *12*(4).

Taborri, J., Agostini, V., Artemiadis, P. K., Ghislieri, M., Jacobs, D. A., Roh, J., & Rossi, S. (2018). Feasibility of muscle synergy outcomes in clinics, robotics, and sports: a systematic review. *Applied Bionics and Biomechanics*, *2018*(3934968).

Tscharner, V. V. (2000). Intensity analysis in time-frequency space of surface myoelectric signals by wavelets of specified resolution. *Journal of Electromyography and Kinesiology*, *10*(6), 433–445.